PAPER

A Fuzzy Geometric Active Contour Method for Image Segmentation

Danyi LI[†a)], ***Nonmember***, **Weifeng LI**[†b)], ***Member***, ***and*** **Qingmin LIAO**[†c)], ***Nonmember***

SUMMARY In this paper, we propose a hybrid fuzzy geometric active contour method, which embeds the spatial fuzzy clustering into the evolution of geometric active contour. In every iteration, the evolving curve works as a spatial constraint on the fuzzy clustering, and the clustering result is utilized to construct the fuzzy region force. On one hand, the fuzzy region force provides a powerful capability to avoid the leakages at weak boundaries and enhances the robustness to various noises. On the other hand, the local information obtained from the gradient feature map contributes to locating the object boundaries accurately and improves the performance on the images with heterogeneous foreground or background. Experimental results on synthetic and real images have shown that our model can precisely extract object boundaries and perform better than the existing representative hybrid active contour approaches.

key words: *geometric active contour, spatial fuzzy clustering, level set method, image segmentation*

1. Introduction

During the last two decades, active contour approaches have received considerable attention and been successfully applied in image segmentation. The basic idea is to evolve a curve and stop it at the desired boundaries of the object through minimizing a given energy function. According to the function's main features, the existing active contour models typically fall into two groups: edge-based models [1]–[4] and region-based models [5]–[9].

The edge-based models utilize the image gradient as their edge stopping function (ESF) to stop the contours on the boundary of the desired objects [2]. Due to the high dependence on localized image information, the model could work well even for heterogeneous foreground or background in certain cases [4]. However, it is sensitive to the noise and weak edges at the same time. Moreover, the edge-based models are prone to obtain a local minimum, which usually leads to unexpected segmentation results.

To avoid these drawbacks, region-based models utilize the statistical information of images instead of the gradients to evolve the contour. One of the most popular models in this category is the Chan-Vese (CV) model [5], and it is successfully applied to binary phase segmentation. Furthermore, a fuzzy region energy has been proposed in [7], where the fuzzy membership is incorporated into the energy function for the sake of providing a strong ability to detect weak boundaries. These region-based models are robust to image noise and can handle objects with weak or smooth edges. However, they often lead to undesired segmentations for the images composed of heterogeneous foreground and background. Meanwhile, because of the absence of local information, it is difficult to locate the boundaries accurately sometimes [8].

To address these issues, [10] introduces a hybrid method, which incorporates geometric curve into the CV method to deal with weak boundaries and heterogeneous background simultaneously. In [11], the fuzzy clustering result is utilized to construct a region-based geometric active contour, which is able to suppress boundary leakages. Moreover, [12] constructs a region-based signed pressure force (SPF) function to substitute the edge stopping function (ESF) in the classical geometric active contour, and it can efficiently stop the contours at weak boundaries.

In this paper, we propose a novel fuzzy geometric active contour method, which combines the process of fuzzy clustering with the evolution of geometric active contour. The evolving curve in every iteration works as a spatial constraint of the fuzzy clustering. Meanwhile, the fuzzy membership is used to construct a region force and incorporated into a geometric active contour. Thus the proposed method can deal with the objects suffered from noise and weak or smooth boundaries efficiently. Moreover, due to the involved local information deduced from the gradient feature map, it is capable of handling the images with heterogeneous foreground and background.

The rest of this paper is organized as follows. In Sect. 2, we review the Fuzzy C-Means (FCM) algorithm and classical geometric active contour model as well as its generalized formula. Section 3 describes the proposed Fuzzy Geometric Active Contour (FGAC) model. The numerical implementation of the proposed model is also summarized in this section. Some experimental results are provided in Sect. 4 to validate the advantages of our model. Section 5 concludes the paper.

2. Background

2.1 Fuzzy C-Means (FCM) Algorithm

In fuzzy clustering, an optimal partition is obtained through minimizing a pre-defined cost function iteratively, which is typically defined to be the weighted distance of the pixels to

Manuscript received November 19, 2012.
Manuscript revised May 23, 2013.

[†]The authors are with the Department of Electronic Engineering/Graduate School at Shenzhen, Tsinghua University, China.
a) E-mail: lidanyi815@sina.com
b) E-mail: li.weifeng@sz.tsinghua.edu.cn
c) E-mail: liaoqm@tsinghua.edu.cn (Corresponding author)

DOI: 10.1587/transinf.E96.D.2107

Copyright © 2013 The Institute of Electronics, Information and Communication Engineers

the cluster center. For a given image I with N pixels to be assigned to c clusters, a classical cost function is defined as follows [13],

$$J_m = \sum_{i=1}^{N}\sum_{j=1}^{c} u_{ji}^m d^2(I(x_i), v_j), \tag{1}$$

where u_{ji} is the membership of pixel x_i in the jth cluster, and v_j is the jth cluster centroid. m controls the fuzziness of the segmentation and $d^2(\cdot,\cdot)$ is a certain distance measure. In order to facilitate the discussion in this paper, we only focus on two-phase problem, i.e., $c = 2$.

By optimizing the object function J_m, the membership matrix u_j and cluster center v_j are updated iteratively:

$$u_{ji} = \frac{1}{\sum_{k=1}^{2}\left(\frac{d_{ji}}{d_{ki}}\right)^{\frac{2}{m-1}}}, \tag{2}$$

$$v_j = \frac{\sum_{i=1}^{N} u_{ji}^m I(x_i)}{\sum_{i=1}^{N} u_{ji}^m}. \tag{3}$$

When the pixels close to their centroids obtain high membership values, and low values for those far-away ones, the cost function J_m is minimized.

2.2 A General Geometric Active Contour Model

Different from FCM which is based on pixel classification, geometric active contours (GAC) utilize the theory of curve evolution for image segmentation. Meanwhile, the level set method is introduced to efficiently solve the curve evolution problem [14]. Suppose that $\phi(x,t)$ denotes the level set function, whose zero set is used to represent the geodesic active contour C, the classical GAC evolves ϕ according to [2]:

$$\frac{\partial\phi}{\partial t} = g(\kappa + V_0)|\nabla\phi| + \nabla g\cdot\nabla\phi. \tag{4}$$

where $\kappa = \mathrm{div}(\nabla\phi/|\nabla\phi|)$ is the curvature, V_0 is a constant velocity term, and g is an edge stopping function (ESF), for instance,

$$g = \frac{1}{1+|\nabla G_\sigma * I|^2}, \tag{5}$$

where $G_\sigma * I$ denotes a smooth version of the given image I with a Gaussian kernel G_σ. Usually, the function g is positive, decreasing and vanishing at object boundaries. In Eq. (4), the evolution speed of ϕ has been tied to g, thus the model can segment images with strong boundaries successfully. However, when the boundaries are not defined by gradient, and appear to be smooth or weak, the classical geometric active contour might leak through these boundaries. In addition, the model is prone to local minimum, failing to converge to the object boundaries with far-away initializations.

In order to solve the aforementioned boundary leaking problem, a signed pressure force (SPF) function [3] using region information is taken into consideration and substitutes for g, and the level set formulation in Eq. (4) is rewritten as follows:

$$\frac{\partial\phi}{\partial t} = (g\cdot\kappa + spf(I(x))\cdot V_0)|\nabla\phi| + \nabla g\cdot\nabla\phi. \tag{6}$$

As pointed out in [3], the SPF function should be constructed to ensure that it has values in the range $[-1, 1]$ and its signs are opposite inside and outside the object. An example is provided in [11], where the result of FCM is utilized to construct the SPF function. The image is classified into two classes, each with a fuzzy membership matrix, then the SPF function is given by

$$spf(I(x)) = 1 - 2u_k(x), \tag{7}$$

where k indicates the ordinal of the interested cluster. This method is found to be helpful for the boundary leaking problem. However, the result of FCMLS method depends on the clustering result of the FCM method directly, when the errors of FCM occur, the FCMLS method will fail.

3. Fuzzy Geometric Active Contour Method

3.1 Description of the Proposed Method

Different from the FCMLS method, which takes advantage of the fuzzy membership deducing from FCM directly, we embed the spatial fuzzy clustering into the evolution of geometric active contour. Let $I : \Omega \to R$ be a given image. The image domain Ω is divided into two subdomains by an evolving curve C: $\Omega_1 = inside(C)$ and $\Omega_2 = outside(C)$. Then our Fuzzy Geometric Active Contour (FGAC) method could be described through the following two procedures:
1. Keeping centroids c_1 and c_2 fixed, we search for the fuzzy membership matrix u_1 and u_2 by minimizing the cost function:

$$J = \sum_{i=1}^{N}\left(u_{1i}^m \parallel I(x_i) - c_1 \parallel^2 + u_{2i}^m \parallel I(x_i) - c_2 \parallel^2\right), \tag{8}$$

2. Keeping fuzzy membership matrix u_1 and u_2 fixed, we search for curve C by the following level set formulation:

$$\frac{\partial\phi}{\partial t} = |\nabla\phi|\left(\mu(u_2 - u_1) + gV_0 + g\mathrm{div}\left(\frac{\nabla\phi}{|\nabla\phi|}\right)\right) + \nabla g\cdot\nabla\phi, \tag{9}$$

where $\|\cdot\|^2$ denotes the l_2-norm, and μ is a constant. c_1 and c_2 express the cluster centers which are the average intensities inside and outside the contour C, respectively.

For a fixed level set ϕ derived from Eq. (9), we can deduce the cluster centers c_1 and c_2 for Eq. (8):

$$\begin{cases} c_1 = \dfrac{\int_\Omega I(x)\cdot H(\phi)dx}{\int_\Omega H(\phi)dx} \\ c_2 = \dfrac{\int_\Omega I(x)\cdot(1-H(\phi))dx}{\int_\Omega(1-H(\phi))dx}, \end{cases} \tag{10}$$

where H is the Heaviside function. Then, with the fixed centroids, the fuzzy membership functions can be updated as a solution of minimizing the cost function J:

$$u_{ji} = \frac{\| I(x_i) - c_j \|^{-2/(m-1)}}{\sum_{k=1}^{2} \| I(x_i) - c_k \|^{-2/(m-1)}}, \ j = 1, 2. \tag{11}$$

Fuzzy clustering methods are successfully applied in pixel clustering. However, they focus on each pixel separately and neglect the spatial information. Therefore, they are sensitive to noise and intensity inhomogeneity. To deal with these issues, we use the evolving curve C as a spatial constraint of the clustering. Comparing the cost function Eq. (8) with Eq. (1), we find that the cluster centers are no longer determined by optimizing J_m iteratively, and they instead depend on the evolving contour C. The average intensities inside and outside C are set to be new centroids in every iteration. Thus, both the intensity information and the spatial information are included in the new centroids, which can provide more robust and accurate clustering.

Moreover, fuzzy clustering, as a tool for soft segmentation, possesses more robust characteristics for ambiguity than other hard segmentation methods. Therefore, the fuzzy membership u_j, which is updated through minimizing J, is utilized to construct the SPF (the first term in Eq. (9)), and its significance can be explained referring to Fig. 1. Because its signs appear to be opposite inside and outside the desired object, the contour shrinks outside the desired object and expands inside. Furthermore, the fuzziness of this force term improves the performance of classical geodesic active contour model on detecting the objects with weak or smooth boundaries. This is illustrated in Fig. 2, where the image is with very smooth boundaries. The classical GAC method leaks through these boundaries as shown in Fig. 2 (b). The involved region term in FCMLS method appear to be helpful for boundary leaking problem but not adequate as shown in Fig. 2 (c). Comparatively, Fig. 2 (d) shows the result of

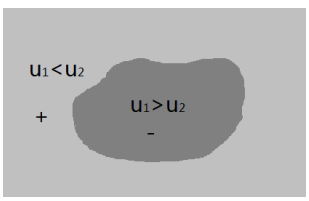


Fig. 1 We assume that the dark object denotes the 1st cluster, and the signs of the fuzzy region force inside and outside the object are opposite.

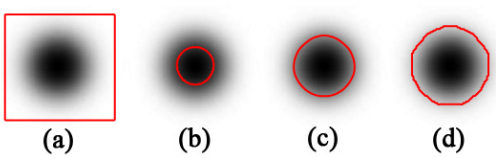


Fig. 2 Comparisons between our model with GAC and FCMLS method on a synthetic image with very smooth contour. (a) initial contour; (b) the result of GAC method; (c) the result of FCMLS method. (d) the result of our method.

the proposed method, and the smooth boundary is detected more accurate than the other two methods. This demonstrates the effectiveness of the novel force term in Eq. (9) for the weak or smooth boundaries.

Subsequently, the other three terms in Eq. (9) are elaborated. The second one is a constant velocity term which is used to increase the evolving speed. The role of the third curvature term is to smooth and regularize the contour, and the weight g weakens its effect at well-defined boundaries. The last term acts as an attractive force to attract the curve C to the real boundaries. When the gradient variations are small, the first three terms play an important role in attracting the curve to the boundaries. Therefore, the model is robust to noise and can handle weak or smooth boundaries. When the curve is close to object boundaries, the last term is dominant to attract the curve to boundaries. In such a way, the boundaries are accurately located with the assistance of the local information.

In summary, our method possesses the following properties: (1) Our model embeds the process of fuzzy clustering into the evolution of geometric active contour, and the evolving curve works as a spatial constraint of the clustering in every iteration. It is worth noting that, the fuzzy region term of FCMLS in Eq. (7), which is deduced from the FCM method directly, is invariable in the curve evolution. (2) The fuzzy region term provides our model the ability to avoid leakages at weak boundaries and robustness to the noises; (3) The edge-based term related to the image gradients contributes to locating the object boundaries accurately and handling the images with heterogeneous foreground or background.

3.2 Implementation

To avoid re-initialization [15], which is utilized to keep the level set function smooth near its interface, we adopt the Selective Binary and Gaussian Filtering Regularized Level Set (SBGFRLS) method introduced in [12] to implement the evolution in Eq. (9). According to [12], the curvature term κ could be removed, and instead a Gaussian kernel filter is introduced to regular the level set function [9], [16]. Thereupon, the level set formulation of our FGAC method can be rewritten as,

$$\frac{\partial \phi}{\partial t} = |\nabla \phi| \left(\mu(u_2 - u_1) + gV_0\right) + \nabla g \cdot \nabla \phi. \tag{12}$$

Finally, the procedures of the proposed method could be summarized as illustrated in Algorithm 1.

Note that, step 7 of the algorithm is a selective procedure, and it should be implemented when the local segmentation property is demanded, thus only the points near the interface will evolve. It provides the feasibility to segment the object selected by the initial contour and can deal with the images corrupted by intensity inhomogeneity. Otherwise, if the task is to detect all the objects, this step should be removed.

Algorithm 1 Segmentation using our fuzzy geometric active contour (FGAC) method.

Input: input image I, initialization level set function ϕ_0, the standard deviation σ of the Gaussian filter, time step τ, maximum iteration number N.

Output: level set function ϕ, segmentation result.

1: Initial the level set function $\phi^1 = \phi_0$.
2: **for** $k = 1$ to N **do**
3: Fix ϕ^k, calculate the cluster centers c_1^{k+1} and c_2^{k+1} from Eq. (10);
4: Update u_1^{k+1} and u_2^{k+1} from Eq. (11);
5: Calculate the gradient descent flow $\frac{\partial \phi}{\partial t}$ by Eq. (12);
6: Update the level set function $\phi^{k+1} = \phi^k + \tau \frac{\partial \phi}{\partial t}$.
7: Let $\phi^{k+1} = 1$ if $\phi^{k+1} > 0$, and $\phi^{k+1} = -1$ otherwise.
8: Regularize ϕ with a Gaussian filter: $\phi^{k+1} = \phi^{k+1} * G_\sigma$
9: **if** $\phi^{k+1} == \phi^k$ **then**
10: break iteration.
11: **end if**
12: **end for**
13: Output $\phi = \phi^{k+1}$, and extract the object according to ϕ.

4. Experimental Results

In this section, the experiments are carried out in order to demonstrate the effectiveness of our method in handling noise, weak boundaries and heterogeneous foreground or background in both synthetic and real images. The parameters of our method for all the test images are $\tau = 1$, $\sigma = 1$, $N = 500$, and V_0 is set to 0.6 in all experiments unless otherwise stated. μ and m are tuned so as to fit different images.

4.1 Selection of Parameters

In this subsection, we demonstrate the influence of different μ and m values on the final results.

First, the weight of the fuzzy region force μ impacts the capture capability of curve evolution. If we intend to detect as many objects as possible, then μ has to be large. If only large objects need to be detected, then μ should be smaller. These are demonstrated in Fig. 3, and the global segmentation property is utilized in this experiment. When μ is small, the contour cannot flow into narrow regions such as the gaps between balls in Fig. 3, and only large objects are detected, or objects formed by clustering as shown in Fig. 3 (b). In contrast, a larger μ will increase the expending or shrinking capability of the evolution curve, and the objects of any size tend to be detected as shown in Fig. 3 (c). Moreover, it could be observed that our model allows for the change of topology automatically.

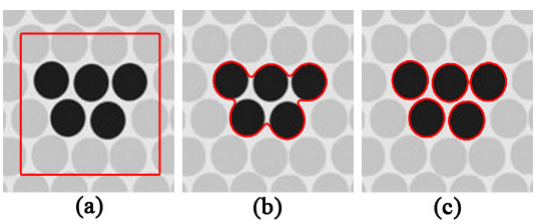


Fig. 3 Detection of geometrically similar objects with different parameter μ. (a) initial contour; (b) the result of our method by setting $\mu = 0.5$, $m = 4.0$; (c) the result of our method by setting $\mu = 3.0$, $m = 4.0$.

Secondly, the parameter m impacts the detection of weak boundaries. Typically, the weaker the boundaries are, the larger value the parameter m takes. This is illustrated in Fig. 4, and local segmentation property is utilized. The background intensities of Figs. 4 (a) and (b) are both 127. The intensities of the 1st and 2nd part in Fig. 4 (a) are 90 and 0, respectively. Meanwhile, the intensities of the 3rd and 4th part in Fig. 4 (b) are 105 and 0, respectively. In Fig. 4 (a), we want to detect the rectangle, whose left-most boundary is weaker than its adjacent fake boundary inside the object. Therefore, with a small parameter $m = 2$, the contour passes over the relatively weaker part of the object, and when we adopt larger parameter $m = 4$ or 6, the evolving curve can effectively stop at the weak boundary. Figure 4 (b) presents a synthetic rectangle, whose left-most boundary is even weaker than that of Fig. 4 (a). Thus, with $m = 4$, there is also boundary leaking problem, and a larger parameter $m = 6$ solves the problem successfully.

4.2 Analyzing the Region and Edge Based Force

In this subsection, we compare our method with its counterpart without the fuzzy region force, that is geometric active contour (GAC) method, and also the counterpart without the edge based term, to demonstrate the importance of the fuzzy term and edge based term, respectively. The local segmentation property is utilized for all the images in this subsection.

In Fig. 5, the intensity is nonuniform over the duck's body. Thus the fuzzy term without gradient information cannot detect the darker part such as duck's bill and wing as shown in Fig. 5 (b). The GAC method can deal with heterogeneous foreground owing to the involved local information, however the shadows near the duck trap the contour into an undesired local minimum (see Fig. 5 (c)). Comparatively, our method achieves more accurate segmentation result as shown in Fig. 5 (d). On one hand, the edge-based force provides the capability to handle heterogeneous foreground; On the other hand, the fuzzy region force plays an important role in driving the evolving curve away from local minima and turning to converge to the desired boundaries accurately.

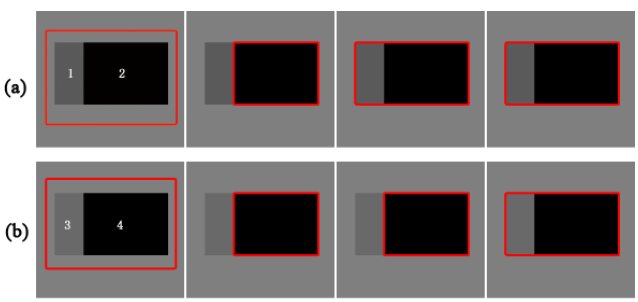


Fig. 4 Detection of objects with weak boundaries by setting different parameter m. First column shows the initial contours. The segmentation results of our method by setting $m = 2$, 4 and 6 are shown in the second, third and last column, respectively. μ is set to be 1.0.

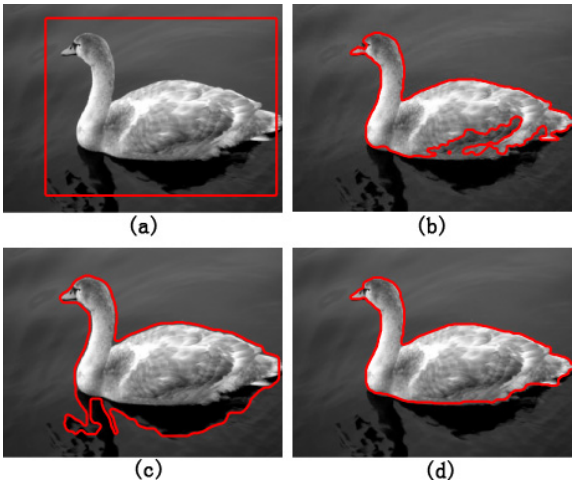


Fig. 5 Detection of the duck corrupted by intensity inhomogeneity. (a) initial contour; (b) the result of our method without the edge based term; (c) the result of our method without the fuzzy region force (that is GAC method); (d) the result of our method by setting $\mu = 1$, $m = 4$.

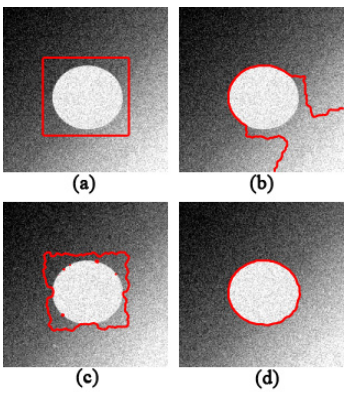


Fig. 6 (a) initial contour; (b) the result of our method without the edge based term; (c) the result of our method without the fuzzy region force (that is GAC method); (d) the result of our method by setting $\mu = 2$, $m = 6$.

Another example is provided in Fig. 6, where the image is corrupted by intensity inhomogeneity and noise. Due to the global region information involved in the fuzzy region force, it cannot deal with intensity inhomogeneity alone, and the brighter part of background is detected undesirably (see Fig. 6 (b)). Because the curve evolution of GAC method depends on the gradient information, which is sensitive to the noises, it cannot achieve satisfying segmentation as shown in Fig. 6 (c). Owing to the capability of handling intensity inhomogeneity provided by the edge-based force, and the robustness to noise provided by the fuzzy region force, our model can obtain satisfying result as shown in Fig. 6 (d) ($V_0 = 3.0$).

4.3 Comparison Experiment

The comparisons are implemented between our method with the FCMLS method [11] and Selective Local or Global segmentation (SLGS) method [12]. These two methods both introduce region information into the classical GAC model through constructing SPF functions. The SPF function involved in the FCMLS method takes advantage of the fuzzy membership deduced from FCM directly, and that of the SLGS method is based on the intensity averages inside and outside the evolving curve. All the methods use the same initializations for fairness. Meanwhile, the parameters for the compared methods are set after we tune and select best ones. The local segmentation property of our method is utilized for all the images in this subsection.

Table 1 Errors (in percentage) between the ground truth and segmentation results of different methods.

Method	FCMLS	SLGS	Ours
DUCK	31.48	4.54	**2.61**
FISH	66.55	9.94	**3.72**
BOAT	88.01	15.12	**8.76**
EAGLE	65.00	52.33	**2.98**

As shown in Fig. 7, we conduct experiments on four nature images, and Table 1 shows the errors between results by each method and the ground truth [17]. The error [18] is defined as follows,

$$e = 1 - \frac{N(S_1 \cap S_2)}{N(S_1 \cup S_2)}, \tag{13}$$

where S_1 represents the region segmented by the algorithm, S_2 is its corresponding result in the ground truth and $N(\cdot)$ represents the operation of calculating area.

Because the fuzzy membership deduced from the FCM method is utilized to construct the region force of the FCMLS method directly, its segmentation results depend on the clustering results of FCM to some extent. Thus, for the images corrupted by intensity inhomogeneity, the fuzzy memberships of FCM cannot reveal the real object, and the FCMLS method might fail in this case. In the DUCK image, the intensity is nonuniform over the duck's body, and the duck's head and wing are darker than other parts. Only the brighter parts are extracted by the FCM, thus the FCMLS method cannot achieve satisfying segmentation results either. Meanwhile, similar unsatisfying result is presented in the EAGLE image. In the BOAT image, the segmentation of the boat is affected by the heterogenous background, and both the boat and the brighter background, i.e., the water, are extracted by the FCMLS method. Similarly, the inhomogeneous intensity of the background in the FISH image prevents the FCMLS method from meaningful segmentation results.

Due to the selective local segmentation property of the SLGS method, the segmentation results of the DUCK, FISH and BOAT images appear to be more satisfying than the FCMLS method, but not accurate enough when compared with our method. For example, in the FISH image, the gradients along the fins' edges are ill-defined, so the contours extracted by the SLGS method cannot precisely stop at the object boundaries. However, our method prevents the leakages at the weak boundaries more successfully with the assistance of the fuzzy region force, and the segmentation re-

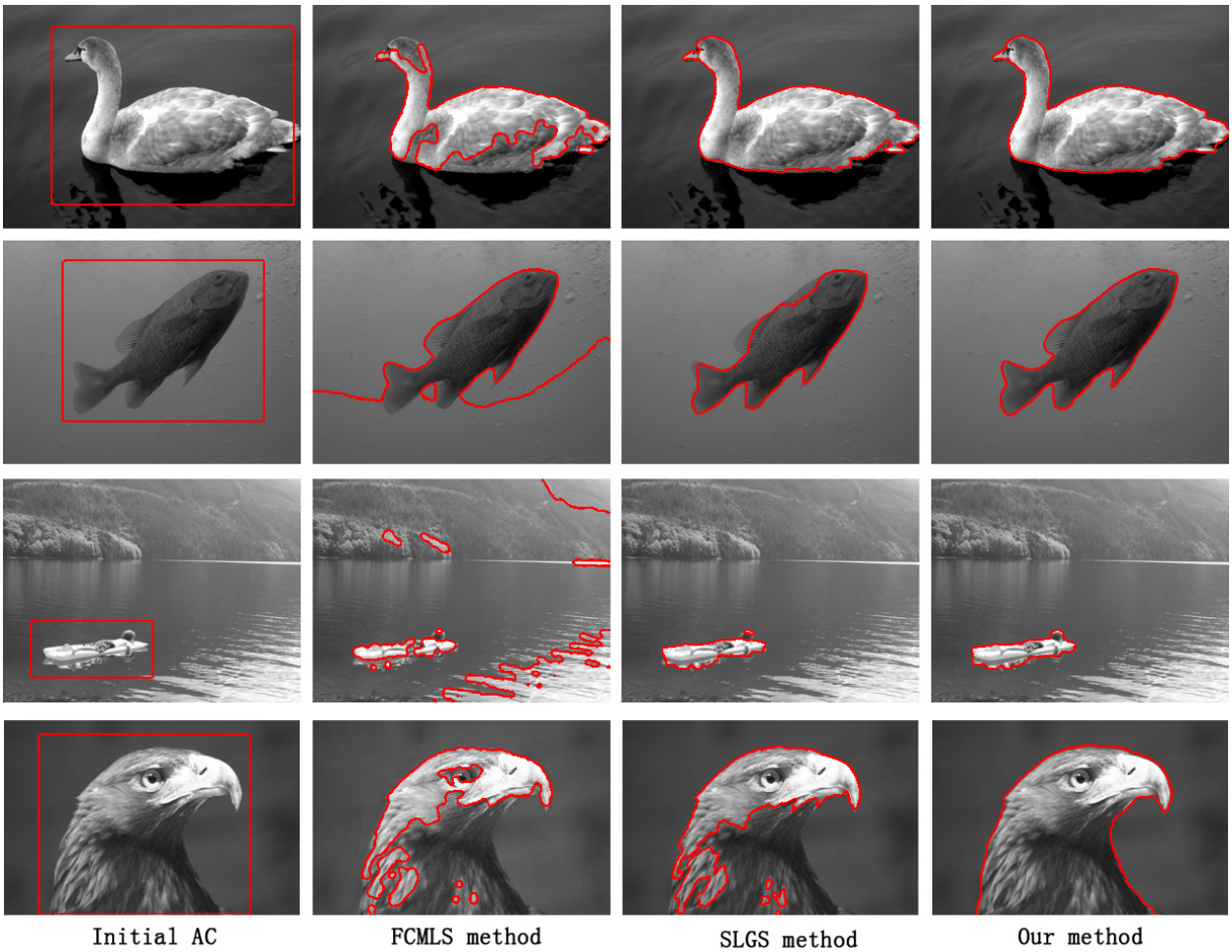


Fig. 7 Detection of object boundaries using FCMLS method, SLGS method and our method on four nature images (DUCK, FISH, BOAT, EAGLE). The parameter μ is set to be 1 for the DUCK, FISH and BOAT image, and be 0.4 for the EAGLE image. m is set to be 4 for the DUCK, FISH image and to be 6 for the BOAT and EAGLE image.

Table 2 Converged iterations by SLGS method and our method.

Image	DUCK	FISH	BOAT	EAGLE
SLGS	360	320	95	350
Ours	**240**	**100**	**60**	**240**

sult appears to be more accurate as shown in Table 1. Because the intensity averages inside and outside the evolving curve are adopted to construct the region force of the SLGS method, it is ineffective in handling images with severe intensity inhomogeneity. Thus, only the brighter parts are extracted in the BOAT and EAGLE images. Comparatively, owing to the capability of detecting the weak edges provided by the fuzzy region force and the local information provided by the edge-based force, our model can obtain satisfying contour from the BOAT and EAGLE images.

The converged iterations for Fig. 7 are compared in Table 2[†]. It can be observed that the proposed method has fewer converged iterations when compared to the SLGS method.

4.4 Robustness to Noises

We generate several noisy images by adding different kinds of noise to the DUCK image as shown in Fig. 8. Figures 8 (a) and 8 (b) are generated with additive "Gaussian" noise of mean 0 and standard deviation 30, "salt & pepper" noise of intensity 0.1 respectively. Figure 8 (c) is generated by adding "speckle" multiplicative noise with standard deviation 70, and Fig. 8 (d) is generated by adding "Poisson" noise. The initial contours used in these four noisy DUCK images are identical with the one for the DUCK image in Fig. 7, and we adopt $m = 6$ for all the noisy images, and μ is set to be 2.0, 1.5, 1.5 and 1.0 for Figs. 8 (a), (b), (c) and (d), respectively. Moreover, V_0 is 1.5 for all the noisy images in this subsection. It can be observed that our method is still able to detect the boundaries of the object accurately.

[†]Because the segmentation results of FCMLS method are far away from the ground truth, we do not list its number of iterations in Table 2.

Table 3 Errors (in percentage) between ground truth and segmentation results shown in Fig. 8.

Image	(a)	(b)	(c)	(d)
FCMLS	31.73	35.88	36.03	32.07
SLGS	7.16	6.05	13.65	5.37
Ours	**5.00**	**3.41**	**3.83**	**2.71**

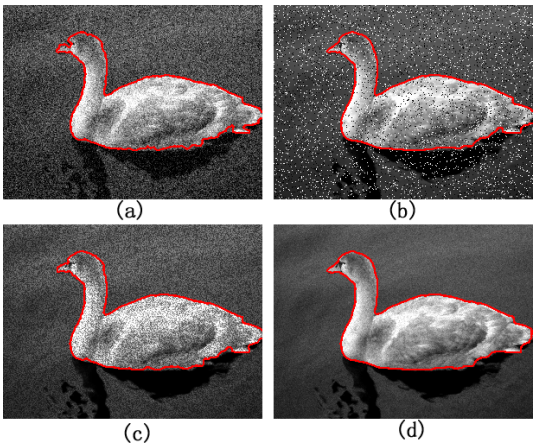


Fig. 8 Detection of object boundaries using our method on the DUCK image corrupted by different kinds of noise: (a) Gaussian noise, (b) salt & pepper noise, (c) speckle noise, (d) Poisson noise.

Furthermore, the errors of our method compared to FCMLS method and SLGS method for the DUCK image corrupted by various noises are measured in Table 3. According to Tables 1 and 3, we find that the proposed method can gain low errors even for the images corrupted by various noises.

5. Conclusion

In this paper, a novel fuzzy geometric active contour method is introduced. It integrates the process of spatial fuzzy clustering with the evolution of geometric active contour. The fuzzy membership is utilized to construct the region driving force, while the cluster centers directly depend on the evolving curve in every iteration. Experimental results demonstrate that the proposed method can better deal with weak edges and heterogenous foreground or background compared with the other two state-of-the-art approaches. Furthermore, the fuzziness involved in the proposed method provides robustness in the presence of various noise.

Acknowledgment

This work is supported by the key joint program of National Natural Science Foundation and Guangdong Province under grant No. U1201257.

References

[1] M. Kass, A. Witkin, and D. Terzopoulos, "Snakes: Active contour models," Int. J. Comput. Vis., vol.1, no.14, pp.321–331, 1987.
[2] V. Caselles, R. Kimmel, and G. Sapiro, "Geodesic active contours," Int. J. Comput. Vis., vol.22, no.1, pp.61–79, 1997.
[3] C. Xu, A. Yezzi, and J. Prince, "On the relationship between parametric and geometric active contours," Proc. 34th Asilomar Conference on Signals Systems and Computers, 2000, pp.483–489, 2000.
[4] A. Mishra and A. Wong, "KPCA: A kernel-based parametric active contour method for fast image segmentaion," IEEE Signal Process. Lett., vol.17, no.3, pp.312–315, 2010.
[5] T. Chan and A. Vese, "Active contours without edges," IEEE Trans. Image Process., vol.10, no.2, pp.266–276, 2001.
[6] T. Brox and D. Cremers, "On the statistical interpretation of the piecewise smooth Mumford-Shah functional," Proc. Scale Space and Variational Methods in Computer Vision, 2007, pp.203–213, 2007.
[7] S. Krinidis and V. Chatzis, "Fuzzy energy-based active contours," IEEE Trans. Image Process., vol.18, no.12, pp.2747–2755, 2009.
[8] S. Lankton and A. Tannenbaum, "Localizing region-based active contour," IEEE Trans. Image Process., vol.17, no.11, pp.2029–2039, 2008.
[9] K. Zhang, H. Song, and L. Zhang, "Active contour driven by local image fitting energy," Pattern Recognit., vol.43, no.4, pp.1199–1206, 2009.
[10] L. Chen, Y. Zhou, Y. Wang, and J. Yang, "GACV: Geometric-aided C-V method," Pattern Recognit., vol.39, no.7, pp.1391–1395, 2006.
[11] B. Li, C. Chui, S. Chang, J. Wu, and S. Ong, "Integrating spatial fuzzy clustering with level set methods for automated medical image segmentation," Computers in Biology and Medicine, vol.41, pp.1–10, 2011.
[12] K. Zhang, L. Zhang, H. Song, and W. Zhou, "Active contours with selective local or global segmentation: A new formulation and level set method," Image Vis. Comput., vol.28, no.4, pp.668–676, 2010.
[13] J. Dunn, "A fuzzy relative of the isodata process and its use in detecting compact well separated clusters," J. Cybernetics, vol.3, no.3, pp.32–57, 1974.
[14] S. Osher and J. Sethian, "Fronts propagating with curvature-dependent speed: Algorithms based on Hamilton-Jacobi formulations," J. Comput. Phys., vol.79, no.1, pp.12–49, 1988.
[15] C. Li, C. Xu, C. Gui, and M.D. Fox, "Level set evolution without re-initialization: A new variational formulation," IEEE Conference on Computer Vision and Pattern Recognition, 2005, pp.430–436, 2005.
[16] Y. Shi and W. Karl, "Real-time tracking using level sets," IEEE Conference on Computer Vision and Pattern Recognition, 2005, pp.34–41, 2005.
[17] S. Alpert, M. Galun, T. Basri, and A. Brandt, "Image segmentation by probabilistic bottom-up aggregation and cue integration," IEEE Conference on Computer Vision and Pattern Recognition, 2007, pp.1–8, 2007.
[18] J. Tohka, "Surface extraction from volumetric images using deformable meshes: A comparative study," Proc. European Conference in Computer Vision, 2002, pp.350–364, 2002.



Danyi Li was born in Harbin, Heilongjiang, China, in 1988. She received the B.E. degree from Department of Electronics and Information Engineering, Harbin Engineering University, Harbin, China, in 2009. She is currently working towards the Ph.D. degree in electronics engineering at Tsinghua University, Beijing, China. Her research interests include applications of medical image processing.



Weifeng Li received the M.E. and Ph.D. degrees in Information Electronics at Nagoya University, Japan in 2003 and 2006, under the guidance of Prof. Fumitada Itakura and Prof. Kazuya Takeda. He joined the Idiap Research Institute, Switzerland in 2006, and in 2008 he move to Swiss Federal Institute of Technology, Lausanne (EPFL), Switzerland as a research scientist. Since 2010 he has been an associate professor in the Department of Electronic Engineering, Graduate School at Shenzhen, Tsinghua University, China. His research interests are in the areas of audio and visual signal processing, Biometrics, Human-Computer Interactions (HCI), and machine learning techniques. He is a member of the IEEE.



Qingmin Liao was born in 1963. He received the B.S. degree in radio technology from the University of Electronic Science and Technology of China, Chengdu, China, in 1984, and the M.S. and Ph.D. degrees in signal processing and telecommunications from the University of Rennes 1, Rennes, France, in 1990 and 1994, respectively. Since 1995, he has been joining with Tsinghua University, Beijing, China. He became Professor in the Department of Electronic Engineering of Tsinghua University, in 2002. From 2001 to 2003, he served as the Invited Professor with a tri-year contract at the University of Caen, France. Since 2010, he has been Director of the Division of Information Science and Technology in the Graduate School at Shenzhen, Tsinghua University, Shenzhen, China. His research interests include image video processing, transmission and analysis; biometrics; and their applications to medicine, industry, and sports. He has published over 90 papers internationally.